JOURNAL OF MATERIALS SCIENCE 9 (1974) 121–128

Temperature dependence of yielding and work-hardening rates in magnesium oxide single crystals

M. SRINIVASAN, T. G. STOEBE
Division of Metallurgical Engineering, University of Washington, Seattle, Washington, USA

The mechanical properties of MgO single crystals have been analysed for their yielding and work-hardening behaviour as a function of purity and deformation temperature. The Fleischer theory accounts for the observed temperature dependence of the critical resolved shear stress well. Depending on temperature and impurity content, the MgO single crystals are shown to exhibit two-stage work-hardening behaviour, with the hardening shown to be athermal in nature. At and below room temperature, a temperature-dependent contribution results from dislocation-point defect interactions, while the primary athermal contribution arises out of dislocation-dislocation dipole interactions. The CRSS and work-hardening behaviour of MgO single crystals indicates a close relationship to the deformation characteristics of NaCl-structure alkali halides.

1. Introduction

It is generally known that the yielding behaviour in ionic solids is governed by the resistance offered by the impurities to the motion of freshly introduced dislocations. In impure crystals of MgO, the temperature dependence of the yield stress has been studied by several workers [1-5]. However, apart from the work of Moon and Pratt [5], the other workers do not define clearly the heat-treatment procedures used for the crystals, which is very important since heat-treatments markedly influence the state and nature of the impurity dispersion which, in turn, are very important in understanding mechanical behaviour. In addition, the understanding of work-hardening in MgO cannot be considered complete unless the relative contributions of the thermal and athermal components to work-hardening are known and understood. Earlier, the authors have reported a two stage work-hardening in MgO at room temperature [6]. In the light of the available results regarding work-hardening in other systems of the NaCl type crystal structure, principally NaCl [7] and LiF [8] the current study has been undertaken to determine the influence of temperature and impurity content on both yielding behaviour and work-hardening rates in MgO single crystals.

2. Experimental procedure

2.1. samples

Single crystals of magnesium oxide were obtained from the Oak Ridge National Laboratories (ORNL) and from the Norton Company. The following nomenclature is adopted for the different crystals used in the present work: ORNL crystals are the purest available and are denoted as PA; the two different Norton crystals contain varying amounts of impurities and are referred to as NA and NC. A spectrographic analysis of these crystals is given in Table I.

TABLE I Semi-quantitative spectrographic analysis of MgO single crystals, reported as oxides of the elements indicated*

Element	PA	NA	NC
Fe (%)	0.005	0.02	0.01
Si (%)	0.007	0.01	0.015
Mn (%)	0.001	0.002	0.001
Al (%)	0.007	0.02	0.07
Cu (%)	0.0005	0.0005	0.0005
Ca (%)	0.005	0.015	0.25

*Performed by American Spectrographic Laboratories Inc, San Francisco.

2.2. Specimen preparation

After initially sawing the crystals roughly to size, a cleaving machine was used to cleave the

specimens along {100} faces to their final dimensions of approximately 8 × 2.5 × 2.5 mm³. During the entire specimen preparation procedure, care was exercised to introduce minimum surface damage to the crystals, so that reproducible results could be obtained. Tweezers with their ends covered by electrical tape were used to handle the crystals during all phases of the work.

To establish the yield stress of crystals containing a minimum of Fe^{+3}, all of the crystals were given reducing heat-treatment [9]. This treatment consisted of heating the crystals at 2000°C for 2 h in a carbon element furnace with an argon atmosphere. In addition to reducing the iron impurities to Fe^{+2} [6], this treatment also served to standardize the specimens and anneal out any damage caused during the crystal preparation.

2.3. Experiments

All experiments in this investigation have been carried out by compressing the crystals along the long (001) direction, using a compression jig similar in design to that of Pascoe *et al* [10]. The jig could be attached to the crosshead of the Instron Machine, in which for high temperature tests, a nichrome-wound furnace was installed. The furnace was controlled using a Leeds and Northrup Electromax C.A.T. temperature controller, which allowed the sample temperature to be controlled to within ±5°C. The temperature of the sample was monitored using a chromel-alumel thermocouple touching one of the sample faces. After the temperature stabilization the specimen was soaked at temperature for 1 h prior to deformation. Three to four samples each were tested at room temperature, 473, 673 and 873 K.

A low temperature jig of a similar design [10] was used for tests below room temperature. This jig fits into a dewar flask which can contain a liquid coolant. The temperatures obtained were 77 K (liquid nitrogen), 125 K (isopentane liquid) and 195 K (dry ice and acetone). For 125 K, isopentane was contained in a can in which a copper coil was immersed, and the whole arrangement was contained in a liquid nitrogen bath in a dewar flask; air was passed through the copper coil to heat the isopentane to 125 K. Three to four samples were tested at each of these temperatures, the results being reproducible to within 10%. The CRSS is taken as the 0.1% proof stress in the stress-strain curve at a given strain.

The various contributions to work-hardening may be separated using strain-rate change experiments. If m^* is assumed to be independent of strain, and if the dislocation density and internal stress remain constant during a strain-rate change, the effective stress τ^* can be evaluated from the experimental data using the relation [11],

$$\tau^* = \frac{m^*}{m'} \cdot \tau_a \qquad (1)$$

where τ_a is the applied stress, m' is the change in the logarithm of the strain-rate with the change in the logarithm of the stress and m^* is the value obtained by extrapolating m' to zero strain. Strain rates $\dot{\epsilon}$ of 5×10^{-2} to 5×10^{-4} min^{-1} were used. The instantaneous change in strain-rate was made possible by the use of pushbutton cross-head speed selector in the Instron machine. Once τ^* is thus known, the internal stress τ_μ is obtained from the relation, $\tau_\mu = \tau_a - \tau^*$. This is carried out in more detail in a subsequent publication [12].

3. Results

3.1. Stress-strain characteristics

Fig. 1 shows the typical stress-strain characteristics of PA crystals deformed between 77 and 673 K. Slip is generally seen to be most difficult at 77 K and only about 5% plastic strain is achieved at this temperature. 10% plastic deformation is observed for deformation above room temperature for these crystals depending on sample perfection. Slip-band intersection, which may be observed using stress birefringence [13], initiates cracks above 10% strain which propagate through the crystal for catastrophic failure.

Although not very apparent in Fig. 1, two work-hardening stages can be resolved for most of these deformation temperatures, with stage I occurring below 3 to 4% strain after which the work-hardening increases slightly to what could be termed stage II. At a strain-rate of 2.38×10^{-3} min^{-1}, the work-hardening rate taken at 2% strain for stage I, θ_I, is $1.58 \times 10^{-3}\mu$ where μ is the shear modulus of MgO at room temperature; θ_{II} for stage II taken at 6.5% plastic strain is $2.12 \times 10^{-3}\mu$. In comparison, LiF shows two-stage work-hardening behaviour only above room temperature [8] and in LiF at 383 K, the values obtained are $\theta_I = 0.56 \times 10^{-3}\mu$ and $\theta_{II} = 2.1 \times 10^{-3}\mu$. The occurrence of two stages

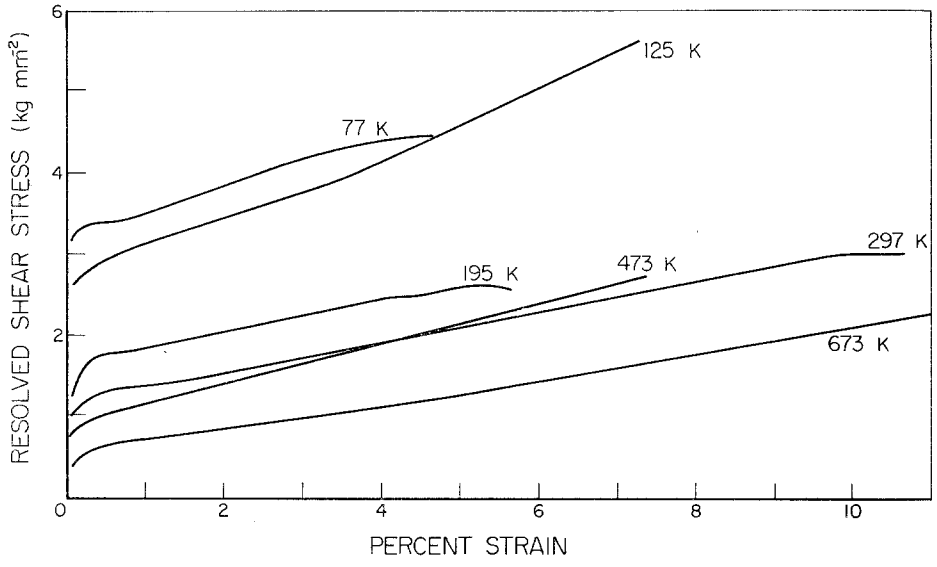

Figure 1 Stress-strain characteristics of PA crystals at various deformation temperatures, as noted.

of work-hardening is independent of the cross-sectional geometry of the samples used, in agreement with earlier work [13].

NA crystals were also compressively deformed at 125 to 673 K. Deformation of these crystals at 77 K was extremely difficult, and despite the use of many crystals of perfect condition, only critical resolved shear stress (CRSS) values could be obtained since the crystals fracture immediately after yielding. This is probably owing to the fact that the yielding value is high enough to generate massive slip on orthogonal slip planes which intersect to initiate and propagate cracks catastrophically immediately after yielding [14]. No two-stage work-hardening behaviour can be identified for these NA crystals at any temperature, and these crystals are less plastic than PA crystals at all temperatures. In case of NC crystals also low temperature deformation was extremely difficult, and stress-strain curves could not be obtained at 77 or at 125 K. These NC crystals are less plastic than either NA or PA crystals, and as in NA crystals, no identifiable two-stage work-hardening behaviour is observed.

3.2. Temperature dependence of the critical resolved shear stress

Fig. 2 shows the effect of temperature on the CRSS of the three types of MgO single crystals used in the current investigation. The CRSS is generally seen to decrease with increasing temperature, the rate of decrease being fastest below room temperature. Using this plot, the CRSS can be separated into two components, τ^*, the short range (thermally activated) stress, and τ_μ, the long range (athermal) component. τ_μ may be obtained from the temperature-independent portion of the CRSS-temperature curve, which for PA crystals yields $\tau_\mu = 0.48$ kg mm^{-2}. This method is rather inaccurate, but above 800 K, the CRSS increases in MgO owing to dynamic strain ageing precluding higher temperature determinations [15]. By a similar analysis for NA crystals, τ_μ yields a value of 1.15 kg mm^{-2}, while for NC crystals, the value is 1.5 kg mm^{-2}.

The relationship between the temperature and the short range or effective stress, τ^*, determined from the temperature dependent portion of Fig. 2 may be used in the hardening model of Fleischer [16, 17]. This model gives a relationship involving the effective stress τ^*, the temperature where $\tau^* = 0$, T_0, and the effective stress at 0 K, τ_0^*, as follows:

$$\frac{\tau^*}{\tau_0^*} = \left[1 - \left(\frac{T}{T_0}\right)^{\frac{1}{2}}\right]^2. \quad (2)$$

Thus a plot of τ^* versus T should be linear, with τ_0^* and T_0 being obtained from the intercepts with the co-ordinate axes. Fig. 3 shows such a plot for the present data, where Equation 2 is seen to be well obeyed with the possible exception of the NC crystals. The analysis for PA

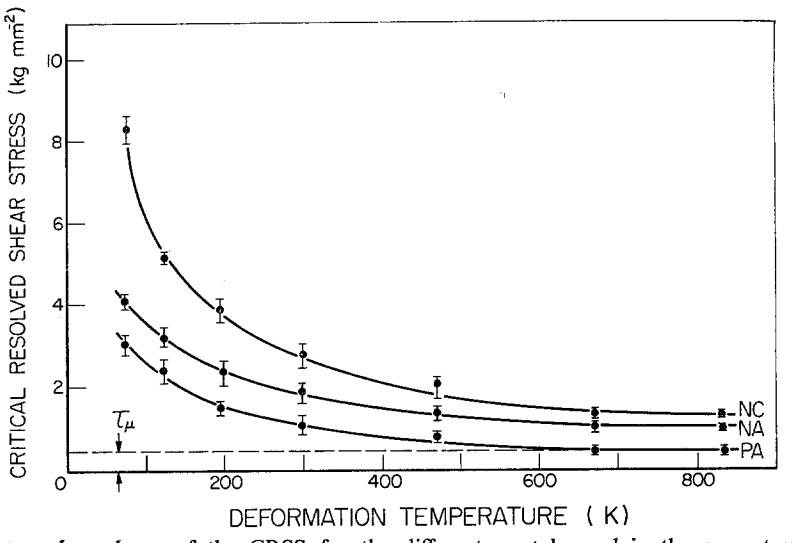

Figure 2 Temperature dependence of the CRSS for the different crystals used in the current study. From the figure, the critical temperature T_0 can be estimated to be between 675 and 875 K; for PA crystals, $\tau_\mu = 0.48$ kg mm^{-2}.

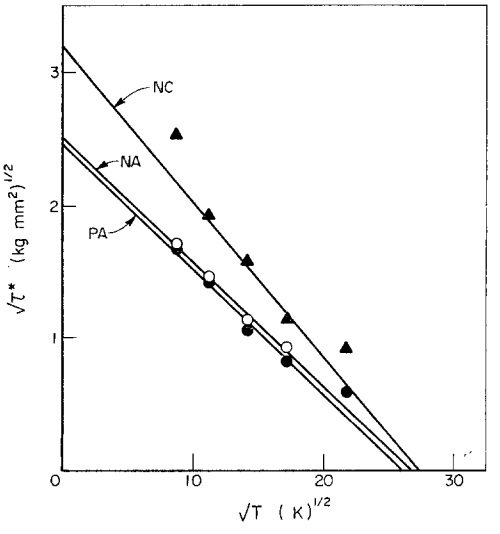

Figure 3 Fleischer plot for the different crystals utilizing the data from Fig. 2.

crystals give $T_0 = 685$ K and $\tau_0^* = 6.0$ kg mm^{-2}; for NA crystals, $T_0 = 715$ K and $\tau_0^* = 6.32$ kg mm^{-2} and for NC crystals, $T_0 = 750$ K and $\tau_0^* = 10.24$ kg mm^{-2}. This increase of τ_0^* with increasing impurity concentration is expected from this model, while T_0 should be nearly temperature independent [18]. The values given are valid to within approximately 10%.

3.3. Temperature dependence of work-hardening rates

Temperature dependence of the observed work-hardening rates normalized in terms of the shear modulus μ, is tabulated in Table II and shown graphically in Fig. 4 for the different MgO crystals used in these experiments. The work-hardening rates have been calculated at particular strains from stress-strain curves. Stage I hardening in PA crystals decreases on warming from 77 K to a plateau just above room temperature, then decreases further; the decrease in stage II above room temperature is similar to that for stage I. For both NA and NC crystals, the one work-hardening rate observed is higher than either θ_I or θ_{II} in the PA crystals after an initial increase; hardening in these crystals shows an initial increase, then decreases above room temperature.

3.4. Estimation of thermal and athermal stress components

The results of strain-rate cycling tests are shown in Fig. 5a to e for five of the temperatures tested. The results indicate that in this system, generally strain hardening results only of athermal stresses, τ_μ, arising from dislocation interactions with obstacles possessing long range stress field. Other aspects of these particular results are discussed in a separate paper [12].

TABLE II Average work-hardening rates and the value calculated for the shear modulus, μ, at temperature indicated

Temperature (K)	$\mu \times 10^{-4}$ (kg mm^{-2})	θ_I @ 2% strain $\times 10^3\ \mu^{-1}$			θ_{II} @ 6% strain $\times 10^3\ \mu^{-1}$			Average % strains to fracture		
		PA	NC	NA	PA	NA	NC	PA	NA	NC
77	1.32	2.63	absent	absent	absent	absent	absent	4.8	0.4	0.38
125	1.31	2.52	absent	absent	3.44	absent	absent	7.25	3.9	0.3
195	1.3	2.07	2.48	3.62	absent	absent	absent	5.75	3.2	6.8
298	1.27	1.55	3.53	4.27	2.01	absent	absent	10.8	7.8	4.1
473	1.23	1.68	2.49	3.99	2.04	absent	absent	7.5	5.0	4.8
673	1.18	1.13	2.28*	1.78*	1.52†	absent	absent	11.6	6.9	7.2

*θ_I @ 3% strain.
†θ_{II} @ 8% strain.

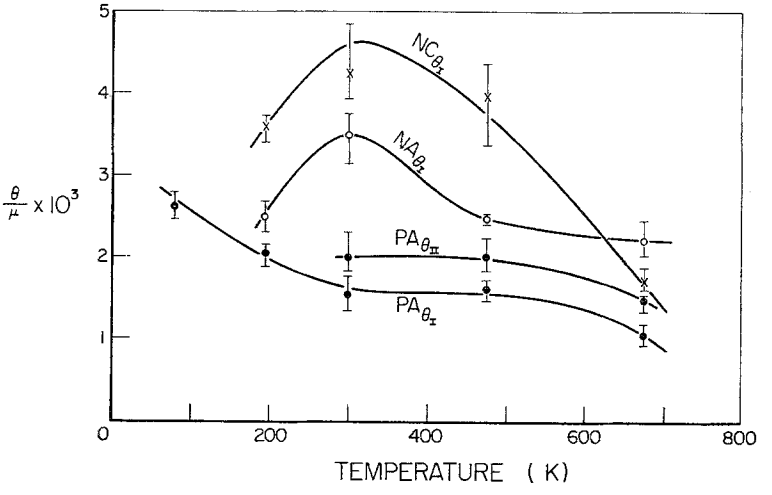

Figure 4 Work-hardening rates, θ_I and θ_{II}, in MgO single crystals as a function of temperature, normalized by the shear modulus, μ.

4. Discussion

4.1. Critical resolved shear stress

In ionic solids, including MgO, the CRSS is governed by the stress required to move the fresh dislocations introduced during the deformation [19], and the resistance to the motion of dislocations is provided by impurities [8, 20]. The MgO single crystals used here contain varying amounts of impurities, as given in Table I. Any of the impurities existing in solid solution in a trivalent state such as Al^{+3} will introduce vacancies into the lattice to maintain electrical charge balance. These vacancies form impurity-vacancy dipoles and dipoles aggregates which are present in various forms depending on temperature [21]. Impurity-vacancy aggregates themselves are generally considered as long range obstacles, while impurity-vacancy dipoles which are rigid in the lattice should have a short range interaction [22].

In Fleischer's model, which has been used in Section 3.2 above, the vacancy-impurity dipole is treated as a rigid defect having a tetragonal symmetry. The short range nature of dislocation-impurity-vacancy dipole leads to a strong temperature dependence of the yield stress, since the dislocation may be activated thermally around the obstacle. Recently, it has been shown that Fleischer's model accounts well for the observed temperature dependence of the flow stress in high purity LiF crystals [23, 24]. Fig 3 shows that Fleischer's model also successfully accounts well for the temperature dependence of the flow stress in MgO.

The assumption in Fleischer's theory that the impurity-vacancy dipole is a rigid defect has

been found to be invalid at high temperatures, since the relaxation time for reorientation of the dipoles becomes relatively small in a number of ionic systems [25]. The interaction between moving dislocations and dipoles can cause the dipole to reorient in the strain field of the dislocations so as to lower the elastic energy of the system [26]. The long range nature of this interaction leads to a strong retarding force, essentially independent of temperature. It is possible that a mechanism similar to this is operative above 600 K, where the CRSS becomes temperature independent.

The disappearance of the temperature-dependent part of the CRSS above about 657°C in PA crystals is indicated by both the direct measurement (Fig. 2) and the Fleischer analysis (T_0 = 685°C). This is further confirmed by the temperature dependence of strain-rate sensitivity ratio which becomes zero near 675°C. Above this temperature, the observed CRSS and work-hardening increase owing to the onset of dynamic strain ageing [15].

4.2. Temperature dependence of work-hardening rates

The current work shows that two work-hardening stages can be resolved in the compressive deformation of MgO single crystals depending on temperature and impurity content. This observation makes the mechanical behaviour of MgO appear to be more closely related to alkali halides of the NaCl type structure than is sometimes thought.

4.2.1. Stage I

Below room temperature the temperature dependent θ_I hardening can be attributed to jog dragging. It has been shown that the kinetics of deformation in MgO are controlled by the slower moving screw dislocations [27]. As the temperature decreases, the dislocation velocity-stress exponent increases, so that the velocity difference between edge and screw dislocations will increase. Thus at low temperature, edge dislocations will move out of the crystal much faster than screw dislocations, leaving a higher density of screw dislocations behind [23]. These will multiply by cross glide, producing a high concentration of dislocation debris, including vacancies and dislocation dipoles.

The results obtained using strain-rate cycling tests indicate that the work-hardening is predominantly athermal in nature (Fig. 5a to e). There is, however, a temperature-dependent contribution to work-hardening arising out of dislocation-vacancy interactions. This is supported by the activation volume measurements made between 77 and 195 K, where V^* seems to be the order of $100b^3$ [12]. The most reasonable activation mechanism for this magnitude of V^* is point-defect dislocation interactions [28]. The high work-hardening rates at these temperatures are, therefore, caused by the high concentration of vacancies produced as a result of the high probability of stress-assisted cross slip which increases continuously with decreasing temperature [29]. This contributes to work-hardening, since some of these vacancies may form monojogs on the dislocation lines, leading to jog dragging [30]. The temperature-independent component of work-hardening may be owing to the production by high jogs of dislocation dipoles having a long range stress field.

In LiF, a dislocation dipole or half loop will shrink by its own force upon isothermal annealing at 100 to 200°C, and will finally annihilate completely [31, 32]. A similar mechanism would become operative at a somewhat higher temperature in MgO. This decrease in dipole concentration is assisted by thermally activated motion of dislocations around these dipole barriers, which becomes considerable at higher temperatures, which would result in a decrease in the observed work-hardening rate. The decrease in the value of θ_I for purer crystals above 473 K may be attributed to this. Thus although "athermal" in nature, work-hardening in MgO is temperature dependent, as in NaCl [7] and LiF [8] owing to the contribution of temperature dependent point defects configurations to work-hardening.

4.2.2. Stage II

Stage II is observed for PA crystals at and above room temperature. The slight increase in work hardening rate over stage I may be attributed to the interaction between dislocations in the primary slip system and those on an intersecting slip system, which act as barriers to dislocation motion in the primary system [6]. Such barriers have been identified in three point bending experiments [33]. In addition, stage II hardening will arise owing to interactions with blocking obstacles and the debris formed on planes inclined to the principal slip plane, as in NaCl [7]. As the temperature increases above room temperature, the work-hardening rate decreases

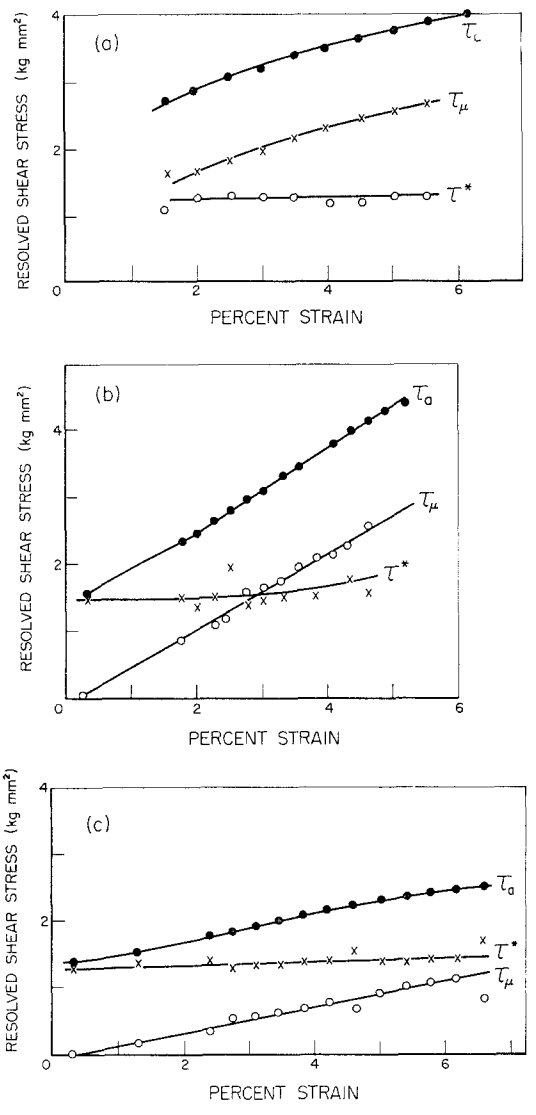

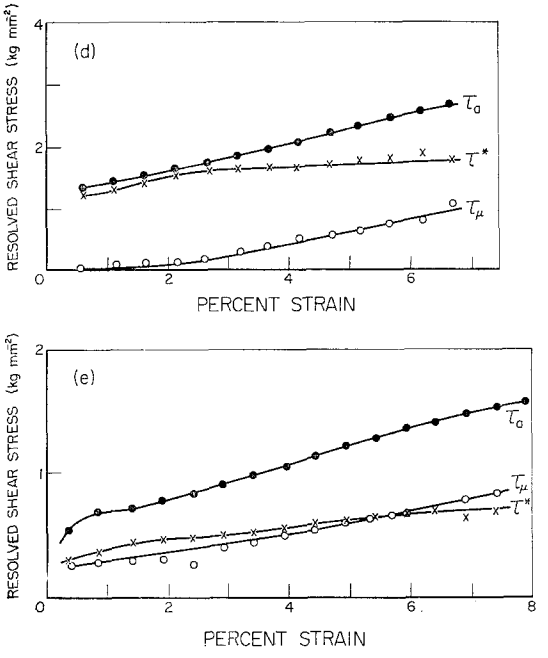

Figure 5 Thermal and athermal components of the flow stress, separated using the strain-rate cycling method at (a) 125 (b) 195, (c) 295, (d) 473 and (e) 673 K.

in the same manner as θ_I. This suggests that the thermally activated mechanism is the same in both stages, except that in stage II, in addition to dislocation dipoles, dislocations in the intersecting slip system become barriers for the dislocation motion in the primary system. Such is also the case in LiF [8].

4.3 Effect of impurities and strain-rate on work-hardening

The Norton crystals, NA and NC, containing varying concentrations of impurities, show single stage work hardening with a hardening rate higher than that of purer crystals. This justification is from the behaviour of stress-strain curves only and other evidences are absent at the present time. A very high work-hardening rate is consistently obtained at room temperature, the cause for which is unknown at the present time (see Fig. 4). The increased hardening compared to purer crystals can be attributed to dislocation-impurity interactions, and the decreased hardening above room temperature can be explained by thermally activated dislocation motion, by breakaway from impurity clouds and which themselves may become less stable at high temperatures.

The inhibition of the two-stage work-hardening behaviour of MgO single crystals by impurities is similar to that reported in LiF [8] and in Ta and Ta alloys [34]. Thus, the isolation of the different stages of work-hardening in a material depends upon the impurity content.

The influence of strain-rate is such that an order of magnitude change in strain-rate causes practically no change in work-hardening rates. The work-hardening rates at the two different strain-rates used is within the range of the error bar shown in Fig. 4. Thus, work-hardening does not depend on the rate of deformation; this again confirms the athermal nature of work-hardening in this system.

5. Conclusions

This work has demonstrated that the overall deformation behaviour of MgO single crystals is closely related to that of alkali halides like NaCl and LiF. The temperature dependence of the CRSS is shown to be explained in terms of Fleischer's theory.

Depending on the temperature and purity of the crystals, the stress-strain curve of MgO single crystals can be resolved to two work-hardening stages; this hardening is shown to be athermal in nature. At and below room temperature there are two contributions to stage I work-hardening, a temperature dependent one rising from dislocation-point defect interactions, and a temperature independent one arising from dislocation-dislocation dipole interactions. Stage II work-hardening may be owing to dislocation interactions with blocking obstacles and the debris formed on planes inclined to the principal slip plane. Above room temperature, the stage I and stage II hardening in MgO behave in a similar manner.

Acknowledgements

Our thanks are extended to Dr Charles Butler of Oak Ridge National Laboratories for supplying the MgO single crystals and to Dr J. Lambert Bates of the Batelle Northwest Laboratories for assistance with the high temperature anneal. Financial support for this work was from the NASA Ceramic Materials Research Program at the University of Washington.

References

1. D. S. THOMPSON and J. P. ROBERTS, *J. Appl. Phys.* **30** (1960) 8.
2. W. L. PHILLIPS, *Trans. Met. Soc. AIME* **218** (1960) 939.
3. C. O. HULSE and J. A. PASK, *J. Amer. Ceram. Soc.* **43** (1960) 373.
4. J. E. MAY and M. L. KRONBERG, *ibid* **43** (1960) 525.
5. R. L. MOON and P. L. PRATT, *Proc. Brit. Ceram. Soc.* **15** (1970) 203.
6. M. SRINIVASAN and T. G. STOEBE, *J. Appl. Phys.* **41** (1970) 3726.
7. A. G. EVANS and P. L. PRATT, *Phil. Mag.* **21** (1970) 951.
8. H. L. FOETDAR and T. G. STOEBE, *ibid* **23** (1971) 859.
9. R. W. DAVIDGE, *J. Mater. Sci.* **2** (1967) 339.
10. R. T. PASCOE, K. C. RADFORD, R. D. RAWLINGS and C. W. A. NEWEY, *J. Sci. Instrum.* **44** (1967) 366.
11. J. C. M. LI, *Canad. J. Phys.* **45** (1967) 493.
12. M. SRINIVASAN and T. G. STOEBE, *J. Mater. Sci.* **8** (1973) 1567.
13. H. L. FOTEDAR, M. SRINIVASAN, D. WILSON and T. G. STOEBE, *Mat. Sci. Eng.* **7** (1971) 272.
14. R. J. STOKES, T. L. JOHNSTON and C. H. LI, *Phil. Mag.* **6** (1961) 9.
15. M. SRINIVASAN and T. G. STOEBE, *J. Mat. Sci. & Eng.* **12** (1973) 87.
16. R. L. FLEISCHER, *J. Appl. Phys.* **33** (1962) 3504.
17. *Idem, Acta Metallurgica* **10** (1962) 835.
18. *Idem, ibid* **15** (1967) 1513.
19. J. J. GILMAN, *Aust. J. Phys.* **13** (1960) 327.
20. W. G. JOHNSTON, *J. Appl. Phys.* **33** (1962) 2175.
21. T. G. STOEBE and P. L. PRATT, *Proc. Brit. Ceram. Soc.* **9** (1967) 181.
22. W. FRANK and A. SEEGAR, Proc. Symp. Interaction Between Dislocations and Point Defects, III, Harwell (1968).
23. H. L. FOTEDAR, Ph.D. Thesis, University of Washington (1971).
24. B. REPPICH, *Acta Metallurgica* **20** (1972) 557.
25. P. L. PRATT, R. P. HARRISON and C. W. A. NEWEY, *Discus. Faraday Soc.* **38** (1964) 211.
26. P. L. PRATT, R. CHANG and C. W. A. NEWEY, *Appl. Phys. Letters*, **3** (1963) 83.
27. A. BRUNEAU, Ph.D. Thesis, University of London (1962).
28. A. G. EVANS and R. D. RAWLINGS, *Phys. Stat. Sol.* **34** (1969) 9.
29. O. V. KLYARIN, A. V. NIKIFOROV, B. I. SMIRNOV and M. YU CHERMOV, *ibid* **35** (1969) 427.
30. U. MESSERSCHMIDT, *ibid* **41** (1970) 549.
31. A. B. DE BELLIS and T. G. STOEBE, *ibid* **10** (1965) K127.
32. F. M. LEE, J. C. SHYNE and W. D. NIX, *Mat. Sci. Eng.* **5** (1970) 179.
33. J. WASHBURN, A. E. GORUM and E. R. PARKER, *Trans. Met. Soc. AIME* **215** (1959) 230.
34. R. J. ARSENAULT and A. LAWLEY, "Work Hardening" (edited by J. P. Hirth and J. Weertman) (Gordon and Breach, New York, 1968) p. 281.

Received 30 March and accepted 6 July 1973.